URSI GASS 2020, Rome, Italy, 29 August - 5 September 2020

Accuracy assessment of the MUF(3000) nowcasting for PECASUS Space Weather services

D. Sabbagh*(1), P. Bagiacchi(1), and C. Scotto(1)
(1) Istituto Nazionale di Geofisica e Vulcanologia, Via di Vigna Murata 605, 00143, Rome, Italy,
e-mail: dario.sabbagh@ingv.it; carlo.scotto@ingv.it; paolo.bagiacchi@ingv.it

Abstract

The Pan-European Consortium for Aviation Space Weather User Services (PECASUS) is one of the three global Space Weather Centers appointed by the International Civil Aviation Organization (ICAO) to generate Space Weather advisories for aviation users. One of the key operational 24/7 products developed by INGV for the HF domain is the MUF(3000) nowcasting, based on a mapping procedure over Europe, which makes use of the available real-time measurements in different locations, and the Ordinary Kriging method for spatial interpolation. The outputs of this procedure have been analysed during three strong geomagnetic storms, and the results have been compared on the basis of the Root Mean Square Error values obtained between predicted and measured MUF(3000) values at two different test stations. A good accuracy is achieved during the considered storm periods, being the overall Root Mean Square Error values at the test stations less than 2 MHz. However, particular cases show that this method could miss possible sudden ionospheric perturbations, and the effect of erroneous data on the accuracy estimation.

1 Introduction

The Pan-European Consortium for Aviation Space Weather User Services (PECASUS) is one of the three global Space Weather Centers appointed by the International Civil Aviation Organization (ICAO) to generate Space Weather advisories for aviation users. As a partner, the Istituto Nazionale di Geofisica e Vulcanologia (INGV) is in charge to develop Space Weather products for the HF and GNSS domains.

Long distance HF communication is enabled by reflection from the ionosphere, whose variable state can adversely affect HF propagation making the upper part of the HF band unavailable, typically during the late phases of ionospheric storms [1]. The Maximum Usable Frequency (MUF) for a given communication path is the highest HF radio frequency that can be used for communication via ionospheric reflection [2]. As a depression of the MUF prohibits aircraft from accessing the highest frequencies normally available, its monitoring is of crucial interest for aviation applications.

Ionospheric assessment for HF communication is achieved by monitoring the MUF over vertical and oblique paths by means of ionosondes, i.e. HF ionospheric radars whose graphical output is called ionogram. In particular, from a vertical ionogram the MUF(3000) parameter can be obtained, which is the MUF for a radio-link over a standard distance of 3000 km and with reflection point in the ionosphere over the sounding location. The existence of well-established software packages for the automatic scaling of vertical ionograms, such as the ARTIST system [3] and the Autoscala program [4], allows the integration of their output data in real-time to provide nowcasting and short-term forecasting models [5, 6].

One of the key operational 24/7 products developed by INGV for PECASUS is the MUF(3000) nowcasting over Europe. The approach uses advanced Kriging techniques [7], commonly used in the ionospheric field (see, for instance, [8, 9, 10, 11]), and it is based on real-time ionospheric observations. In order to detect possible MUF post-storm depression conditions and issue the corresponding advisories, maps of MUF(3000)/MUF(3000)$_{[bkg]}$ ratio are produced as well, and evaluated by PECASUS forecaster operators.

2 Mapping method

The method here described consists in upgrading background MUF(3000) maps over Europe making use of available real-time measurements from ionosondes located in the considered area. The IRI-CCIR model [12] is used in the whole area as background, being built on monthly median basis. Then, the spatial variable z is defined where measurements are available:

$$z(\boldsymbol{x}_i) = \frac{\mathrm{MUF(3000)}_{[\mathrm{obs}]}(\boldsymbol{x}_i) - \mathrm{MUF(3000)}_{[\mathrm{bkg}]}(\boldsymbol{x}_i)}{\mathrm{MUF(3000)}_{[\mathrm{bkg}]}(\boldsymbol{x}_i)}, \qquad (1)$$

being $\boldsymbol{x}_i$ the geographic coordinates of the *i-th* ionospheric station where measurements are available, and MUF(3000)$_{[obs]}$ and MUF(3000)$_{[bkg]}$ respectively the observed and the IRI-CCIR MUF(3000) values at the desired location (subscripts [obs] and [bkg] stand for 'observed' and 'background', respectively). Once the values of z for a given time are computed, the Ordinary Kriging method [7] is applied for the spatial interpolation over the considered region. Upgraded MUF(3000) maps are then produced over a proper interpolation grid as:

$$\mathrm{MUF(3000)}(\boldsymbol{x}_j) = \left(1 + z(\boldsymbol{x}_j)\right) \cdot \mathrm{MUF(3000)}_{[\mathrm{bkg}]}(\boldsymbol{x}_j), \quad (2)$$

being $\boldsymbol{x}_j$ the geographic coordinates of the *j-th* grid point where the variable z is interpolated. The PECASUS

INGV_MUF_REAL_TIME_15min product applies this method in the region of longitude 12°W-45°E and latitude 32°N-72°N, where the interpolation is performed over a grid with spatial resolution 0.5°x0.5°.
A further PECASUS key product, INGV_MUF_REAL_TIME_RATIO_15min, is also issued by PECASUS in order to immediately detect regions where the modeled real-time MUF(3000) values are lower or greater than the background values. For this purpose, maps of $MUF(3000)_{[ratio]}$ are also built at the same time and in the same region as MUF(3000) maps, being:

$$MUF(3000)_{[ratio]}(\boldsymbol{x_j}) = \frac{MUF(3000)(\boldsymbol{x_j})}{MUF(3000)_{[bkg]}(\boldsymbol{x_j})} = 1 + z(\boldsymbol{x_j}), \quad (3)$$

where MUF(3000) is given by (2). This is particularly useful to define regions of degraded radiocommunication conditions, making use of proper thresholds for the MUF(3000) depression with respect to the background.
Figure 1(a)-(b) shows an example of maps of MUF(3000) and $MUF(3000)_{[ratio]}$ obtained by the described procedure. In this case, data from ionospheric stations of Dourbes (Belgium, 50.1ºN; 4.6ºE), Juliusruh (Germany, 54.6ºN; 13.4ºE), Moscow (Russia, 55.5ºN; 37.3ºE), Pruhonice (Czech Republic, 50.0ºN; 14.6ºE), and Rome (Italy, 41.8ºN; 12.5ºE) are used, while data from Athens (Greece, 38.0ºN; 24.0ºE), Chilton (UK, 51.5ºN; 0.6ºW), Gibilmanna (Italy, 37.9ºN; 14.0ºE), Warsaw (Poland, 52.2ºN; 21.1ºE), and Tortosa (Spain, 40.8ºN; 0.5ºE) ionosondes were not available in real-time. As can be seen in Figure 1(b), slightly degraded radiocommunication conditions occurred over Italy, where a MUF(3000) depression greater than 25% with respect to the background has been obtained.

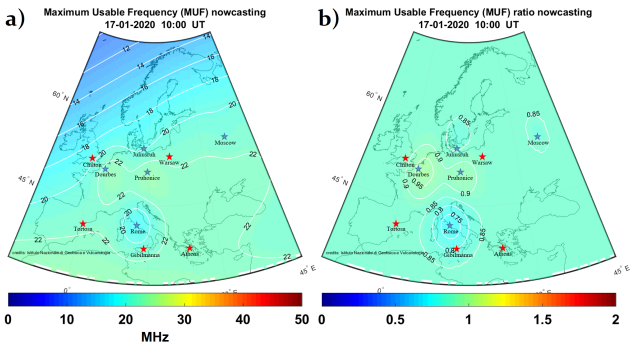

Figure 1. Example of maps of MUF(3000) (a) and $MUF(3000)_{[ratio]}$ (b) obtained by the described procedure. Blue stars represent the ionospheric stations where the data are used, while red stars represents the locations of the ionosondes from where the data were not available in real-time.

3 Case studies analysis

The outputs of the procedure described in Section 2 have been analysed during geomagnetic storm periods in order to assess the reliability of the real-time service. In particular, three strong (G3) geomagnetic storms occurred during March 2012 (case study 1), March 2015 (case study 2), and September 2017 (case study 3) have been analysed. The geomagnetic conditions are assessed based on the K_p index [13] values, according to NOAA Space Weather Scales (https://www.swpc.noaa.gov/noaa-scales-explanation), being K_p=7 the minimum value to be reached during a geomagnetic storm in order to classify it as G3. This threshold corresponds to a value equal to 132 of the geomagnetic index a_p, which is the K_p index expressed in a linear scale [13]. Extended periods (from 6 days for case study 2 up to 13 days for case study 1) with both disturbed and quiet days before and after the main geomagnetic perturbation have been considered for each case study.
MUF(3000) hourly values have been used to test the method, comparing measurements and predictions at the test stations of San Vito (Italy, 40.6ºN; 17.8ºE) and Fairford (UK, 51.7ºN; 1.5ºW). Figure 2(a)-(c) shows, for each case study respectively, the plot of the a_p geomagnetic index during the considered period (upper panel); the plots of predicted $MUF(3000)_{[now]}$ (blue dots, where the subscript [now] stands for 'nowcasting'), observed $MUF(3000)_{[obs]}$ (cyan dots), and their difference $MUF(3000)_{[dev]}=MUF(3000)_{[now]}-MUF(3000)_{[obs]}$ (red dots) for the San Vito (mid panel) and the Fairford (lower panel) ionospheric stations.

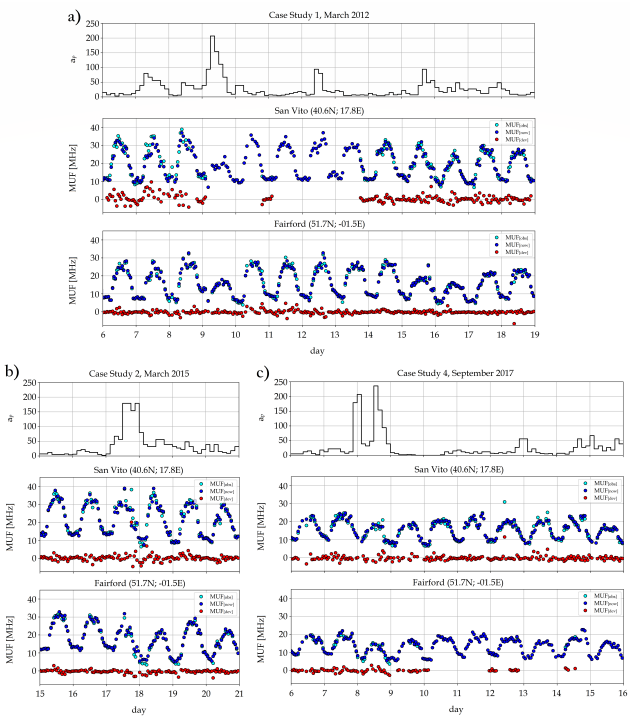

Figure 2. Plots of the a_p geomagnetic index (upper panel); predicted $MUF(3000)_{[now]}$ (blue dots), $MUF(3000)_{[obs]}$ (cyan dots), and their difference $MUF(3000)_{[dev]}$ (red dots) at the San Vito (mid panel) and the Fairford (lower panel) ionospheric stations during the considered periods of the case studies 1 (a), 2 (b), and 3 (c).

As can be seen from subfigures 2(a) and 2(c), some lacks of data occurred for prolonged periods of the case study 1 (from March 9 to 13) from the San Vito ionosonde, and of

the case study 3 (from September 10 to 16) from the Fairford one, for with some sporadic groups of data therein.

The analysis of the results obtained at the station of San Vito highlights the presence of some anomalous $MUF(3000)_{[dev]}$ values (greater than 10 MHz) during cases studies 2 (March 17, 2015, 18.00 UT) and 3 (September 12, 2015, 10.00 UT). As can be seen from Figure 3(a)-(c), an anomalous $MUF(3000)_{[obs]}$ value of 38.19 MHz was recorded on March 17, 2015, 18.00 UT as a consequence of a sudden ionospheric perturbation. This means that, in this case, this method has not been able to follow such a short-time-lived feature.

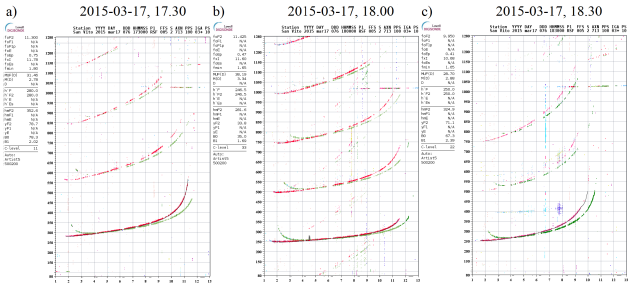

Figure 3. Ionograms recorded by the San Vito ionosonde on March 17, 2015 at 17.30 UT (a), 18.00 UT (b), and 18.30 UT (c).

Instead, the anomalous $MUF(3000)_{[obs]}$ value of 31.02 MHz recorded on September 12, 2017, 10.00 UT is caused by an incorrect autoscaling. Indeed, in this case the autoscaling software failed to correctly recognize the F2 trace of the ionogram, as shown by the incorrect f_0F2 value given as output (Figure 4(b)). This leads to an overestimation also of the MUF(3000) autoscaled value, which results more than 10 MHz greater than the values obtained from the ionograms recorded 15 minutes before (Figure 4(a)) and after (Figure 4(c)).

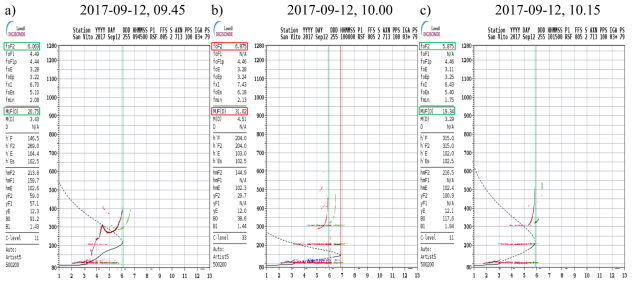

Figure 4. Ionograms recorded by the San Vito ionosonde on September 12, 2017 at 09.45 UT (a), 10.00 UT (b), and 10.15 UT (c). Wrongly autoscaled values are highlighted in red in (b), while correct ones are highlighted in green in all the subfigures.

The results have been compared also on the basis of the Root Mean Square Error (*RMSE*) obtained between predicted and measured MUF(3000) values at the test stations, taking into account the whole data set and each case study separately (Table 1), and only the most disturbed days in each case study (Table 2). In Table 1 the values in brackets are those computed neglecting the September 12, 2017 erroneous autoscaled MUF(3000), while the values in brackets in Table 2 are those computed neglecting the March 17, 2015 anomalous observed value.

Table 1. *RMSE* obtained between predicted and measured MUF(3000) at the test stations of San Vito and Fairford, taking into account the whole data set and each case study separately. The values in brackets are those computed neglecting the September 12, 2017 erroneous autoscaled MUF(3000).

	San Vito		**Fairford**	
	***RMSE* (MHz)**	***n***	***RMSE* (MHz)**	***n***
Case study 1	2.15	184	1.08	291
Case study 2	2.27	138	0.98	127
Case study 3	1.44 (1.17)	188 (187)	0.85	86
Total	1.96 (1.89)	510 (509)	1.02	504

Table 2. *RMSE* obtained between predicted and measured MUF(3000) at the test stations of San Vito and Fairford, taking into account only the most disturbed days of each case study. The values in brackets are those computed neglecting the March 17, 2015 anomalous observed MUF(3000).

	San Vito		**Fairford**	
	***RMSE* (MHz)**	***n***	***RMSE* (MHz)**	***n***
2012-03-09	1.43	3	0.56	19
2015-03-17	4.84 (1.83)	20 (19)	1.27	18
2017-09-08	1.70	16	1.42	17
Total	3.65 (1.75)	39 (38)	1.13	54

As can be seen by the results in Tables 1 and 2, the *RMSE* values obtained at Fairford station are generally lower than those at San Vito. This is an expected result due to the Fairford proximity to the Chilton station, where measurements are assimilated.

The case of March 17, 2015, 18.00 UT shows that this method could miss short-time-lived features when strong geomagnetic perturbations are ongoing, resulting in a possible low accuracy of the MUF(3000) modeling. In this case, the *RMSE* values obtained at San Vito for the case study 2 and only for March 17, 2015 are 2.27 MHz and 4.84 MHz, respectively, while neglecting the anomalous observed MUF(3000) the latter would be considerably lower (1.83 MHz). It should be noted here that March 17, 2015 is the most geomagnetically disturbed day in the case study 2 (maximum a_p=179 – i.e. K_p=8- – Figure 2(b), upper panel), confirming the difficulty of making predictions in adverse Space Weather conditions.

The case of September 12, 2017, 10.00 UT demonstrates instead the effect of erroneous data on the *RMSE* computation. Indeed, the value at San Vito station for the case study 3 would be 1.17 MHz instead of 1.44 MHz, if the erroneous autoscaled MUF(3000) was neglected (in this case, the total *RMSE* value at San Vito results equal to 1.89 MHz, to be compared to the 1.96 MHz value obtained considering the erroneous autoscaled MUF(3000)).

4 Conclusions

The output of the MUF(3000) nowcasting INGV product for PECASUS have been analysed during the three strong geomagnetic storms on March 2012, March 2015, and September 2017, on the basis of the *RMSE* values obtained between predicted and measured MUF(3000) values at the test stations of San Vito and Fairford.
The results obtained at San Vito are more representative of the accuracy of the MUF(3000) modeling than those at Fairford, being the latter very close to the Chilton ionosonde where measurements are ingested. For this reason, all the *RMSE* values obtained at Fairford result lower that the corresponding values at San Vito, confirming a better accuracy achieved at this station. In particular, the overall *RMSE* value obtained at Fairford is equal to 1.02 MHz, while the corresponding obtained over the most disturbed days in each case study is 1.13 MHz.
A good accuracy of the MUF(3000) modeling is achieved during the considered storm periods, being the overall *RMSE* less than 2 MHz (i.e. 1.96 MHz) also at the San Vito test station. This occurs also for the most disturbed day in the case study 3 (September 8, 2017, with *RMSE*=1.70 MHz), while for the whole case study 3 (which is the strongest of the three geomagnetic storms analysed) and the most disturbed day in the case study 1 (March 9, 2012) *RMSE* values result even less than 1.5 MHz (i.e. 1.44 MHz and 1.43 MHz, respectively). These results confirm the good accuracy that could be achieved by this method during strong geomagnetic perturbations, which represent the conditions of greater interest for Space Weather applications. However, the case of March 17, 2015, 18.00 UT shows also that this method could miss short-time-lived features when strong geomagnetic perturbations are ongoing, resulting in a possible low accuracy of the MUF(3000) modeling (*RMSE*=4.84 MHz for that day at San Vito, while *RMSE*=2.27 MHz neglecting the anomalous observed MUF(3000) at 18.00 UT).
The effect of erroneous data on the accuracy estimation is instead highlighted by the case of September 12, 2017, when an incorrectly autoscaled MUF(3000) at 10.00 UT contributes to raise the *RMSE* at San Vito for the case study 3 (1.44 MHz instead of 1.17 MHz neglecting the incorrect MUF(3000) value).
These results demonstrate that the MUF(3000) nowcasting maps over Europe are a state-of-art product and can be used as part of a Space Weather service for real-time assessment of HF radio propagation conditions.

5 Acknowledgements

The authors thank the Lowell DIDBase through GIRO (http://giro.uml.edu/didbase/scaled.php) and the Polish Academy of Science Space Research Centre to provide ionospheric data, and the Kyoto World Data Center for Geomagnetism (http://wdc.kugi.kyoto-u.ac.jp/) to provide geomagnetic data. The Juliusruh data are kindly provided by Leibniz institute of Atmospheric Physics — station Juliusruh, Germany.

6 References

1. “Manual on Space Weather Information in Support of International Air Navigation”. International Civil Aviation Organization, 2018.

2. Davies, K., “Ionospheric Radio”, *Peter Peregrinus Ltd*, London, United Kingdom, 1989.

3. Huang, X., Reinisch, B.W., “Vertical electron density profiles from the digisonde network”, *Adv. Space Res.* **18**, 6, 1996, 121-129.

4. Pezzopane, M., Scotto, C., Tomasik, L., Krasheninnikov, I., “Autoscala: an Aid for Different Ionosondes”, *Acta Geophysica* **58**, 2009, 513-526.

5. Galkin, I.A., Reinisch, B.W., Huang, X., Bilitza, D., “Assimilation of GIRO data into a real-time IRI”, *Radio Sci.* **47**, 2012, RS0L07, doi:10.1029/ 2011RS004952.

6. Mikhailov, A.V., Perrone, L., “A method for foF2 short-term (1–24 h) forecast using both historical and realtime foF2 observations over European stations: EUROMAP model”, *Radio Sci.*, **49**, 2014, 253–270, doi:10.1002/2014RS005373.

7. Kitanidis P.K. “Introduction to geostatistics: application to hydrogeology”, *Cambridge University Press*, Cambridge, 1997.

8. Stanislawska I., Juchnikowski G., Cander L., “The kriging method of ionospheric parameter foF2 instantaneous mapping”, *Ann. Geophys.* **39**, 4, 1996, 845–852. doi:10.4401/ag-4007.

9 Stanislawska I., Juchnikowski G., Cander L., “Kriging method for instantaneous mapping at low and equatorial latitudes”, *Adv. Space Res.* **18**, 6, 1996, 217–220. doi:10.1016/0273-1177(95)00927-2.

10. Liu R.Y., Liu G.H., Wu J., Zhang B.C., Huang J.Y., Hu H.Q., Xu Z.H., “Ionospheric foF2 reconstruction and its application to the short-term forecasting in China region”, *Chin. J. Geophys*. **51**, 2, 2008, 206–213.

11. Pignalberi, A., Pezzopane, M., Rizzi, R., Galkin, I., “Effective solar indices for ionospheric modeling: A review and a proposal for a realtime regional IRI”, *Surv. Geophys.* **39**, 1, 2018, 125–167. doi:10.1007/s10712-017-9438-y.

12. Bilitza, D., “IRI the International Standard for the Ionosphere”, *Adv. Radio Sci.* **16**, 1–11, 2018, doi:10.5194/ars-16-1-2018.

13. Perrone, L., De Franceschi, G., “Solar, ionospheric and geomagnetic indices”, *Annali di Geofisica* **41**, n. 5-6, 1998, 843-855.